Continuous Galerkin methods for solving Maxwell equations in 3D geometries*

Patrick Ciarlet, Jr[1] and Erell Jamelot[2]

[1] POEMS, UMR CNRS-ENSTA-INRIA 2706, ENSTA, 32 bd Victor, 75739 Paris Cedex 15, France, patrick.ciarlet@ensta.fr
[2] Same address, erell.jamelot@ensta.fr

Summary. Maxwell equations are easily resolved when the computational domain is convex or with a smooth boundary, but if on the contrary it includes geometrical singularities, the electromagnetic field is locally unbounded and globally hard to compute. The challenge is to find out numerical methods which can capture the EM field accurately. Numerically speaking, it is advised, while solving the coupled Maxwell-Vlasov system, to compute a continuous approximation of the field. However, if the domain contains geometrical singularities, continuous finite elements span a strict subset of all possible fields, which is made of the H^1-regular fields. In order to recover the total field, one can use additional ansatz functions or introduce a weight. The first method, known as the singular complement method [4, 3, 14, 2, 9, 15, 16] works well in $2D$ and $2D\frac{1}{2}$ geometries and the second method, known as the weight regularization method [13] works in $2D$ and $3D$. In this contribution, we examine some recent developments of the latter method to solve instationary Maxwell equations and we provide numerical results.

1 Introduction and notations

Let $\Omega \subset \mathbb{R}^3$ be a bounded polyhedron with a Lipschitz boundary $\partial\Omega$. In order to simplify the presentation, we suppose that Ω is simply connected and $\partial\Omega$ is connected. Let $\mathbf{n}$ be the unit outward normal to $\partial\Omega$. The boundary $\partial\Omega$ may contain reentrant corners and/or edges, which are called geometrical singularities later on. Let c, ε_0 and μ_0 be respectively the light velocity, the dielectric permittivity and the magnetic permeability ($c \approx 3.10^8$ m.s^{-1}, $\varepsilon_0\mu_0c^2 = 1$). Maxwell equations in vacuum read:

$$\partial_t\mathcal{E} - c^2\,\mathbf{curl}\mathcal{B} = -\mathcal{J}\,/\,\varepsilon_0\,, \tag{1}$$

$$\partial_t\mathcal{B} + \mathbf{curl}\mathcal{E} = 0\,, \tag{2}$$

$$\mathrm{div}\mathcal{E} = \rho\,/\,\varepsilon_0\,, \tag{3}$$

$$\mathrm{div}\mathcal{B} = 0\,. \tag{4}$$

* Submitted to the Proceedings of ENUMATH'05.

Above, $\mathcal{E}$ and $\mathcal{B}$ are the electric field and magnetic induction respectively, ρ and $\mathcal{J}$ are the charge and current densities which satisfy the charge conservation equation:

$$\mathrm{div}\mathcal{J} + \partial_t \rho = 0\,. \tag{5}$$

These quantities depend on the space variable $\mathbf{x}$ and on the time variable t. The boundary is made up of two parts: $\partial\Omega = \overline{\Gamma}_C \cup \overline{\Gamma}_A$, where Γ_C is a perfectly conducting boundary, and Γ_A an artificial boundary. Note that we do not require that $\partial\Gamma_A \cap \partial\Gamma_C = \emptyset$. On Γ_C, we have:

$$\mathcal{E} \times \mathbf{n} = 0 \text{ on } \Gamma_C\,,\ \mathcal{B}\cdot\mathbf{n} = 0 \text{ on } \Gamma_C. \tag{6}$$

Since the choice of the location of Γ_A is free, it is located so that it does not cut nor contains any geometrical singularity [8]. Therefore the tangential trace of $\mathcal{E}$ and the normal trace of $\mathcal{B}$ are regular, and in addition the tangential trace $\mathcal{E}\times\mathbf{n}$ and the normal trace $\mathcal{B}\cdot\mathbf{n}$ vanish near the geometrical singularities. We further split the artificial boundary Γ_A into Γ_A^i and Γ_A^a. On Γ_A^i, we model incoming plane waves, whereas we impose on Γ_A^a an absorbing boundary condition. Both can be modelled [1] as a Silver-Müller boundary condition on Γ_A:

$$(c\,\mathcal{B} + \mathcal{E}\times\mathbf{n})\times\mathbf{n} = c\,\mathbf{b}\times\mathbf{n} \text{ on } \Gamma_A, \text{ where } \mathbf{b} \text{ is given.} \tag{7}$$

In order to solve equations (1-4), with boundary conditions (6) and (7), one needs to define initial conditions (for instance at time $t = 0$):

$$\mathcal{E}(\cdot,0) = \mathcal{E}_0\,,\ \mathcal{B}(\cdot,0) = \mathcal{B}_0, \tag{8}$$

where the couple $(\mathcal{E}_0, \mathcal{B}_0)$ depends only on the variable $\mathbf{x}$.
If we derive (1) in time and inject **curl** of (2) in it, we get a vector wavelike equation for $\mathcal{E}$. We consider then the following equivalent problem (PE): *Find* $\mathcal{E}$ *such that*

$$\partial_t^2\mathcal{E} + c^2\mathbf{curlcurl}\mathcal{E} = -\partial_t\mathcal{J}/\varepsilon_0, \text{ in } \Omega\,,\ t\in]0,T[, \tag{9}$$

$$\mathrm{div}\mathcal{E} = \rho/\varepsilon_0, \text{ in } \Omega\,,\ t\in]0,T[\,, \tag{10}$$

$$\mathcal{E}\times\mathbf{n}_{|\Gamma_C} = 0, \text{ and } (c\mathcal{B}+\mathcal{E}\times\mathbf{n})\times\mathbf{n}_{|\Gamma_A} = c\mathbf{b}\times\mathbf{n}_{|\Gamma_A}\,,\ t\in]0,T[\,, \tag{11}$$

$$\mathcal{E}(.,0) = \mathcal{E}_0, \text{ in } \Omega, \tag{12}$$

$$\partial_t\mathcal{E}(.,0) = \mathcal{E}_1 := c^2(\mathbf{curl}\mathcal{B}_0 - \mu_0\,\mathcal{J}(.,0)), \text{ in } \Omega. \tag{13}$$

The same procedure can be carried out on the magnetic field.

In addition to the usual Lebesgue and Sobolev spaces, the building of the ad hoc variational formulations requires to introduce some non-standard functional spaces [13, 8]. We suppose that Ω has N_{re} reentrant edges of dihedral angles $(\Theta_e = \pi/\alpha_e)_{e=1,\ldots,\mathrm{N}_{re}}$, with $1/2 < \alpha_e < 1$. Let r_e denote the orthogonal distance to the reentrant edge e, and $r = \min_{e=1,\ldots,\mathrm{N}_{re}} r_e$.

Let $L^2(D)$ be the usual Lebesgue space of square integrable functions over D, $D \in \{\Omega, \partial\Omega\}$, and $L^2_\gamma(\Omega)$ be the following weighted space, with $||.||_{0,\gamma}$ norm:

$$L^2_\gamma(\Omega) = \{v \in \mathcal{D}'(\Omega) \,|\, \int_\Omega w(r)\, v^2 \,\mathrm{d}\Omega < \infty\}\,,\ ||v||^2_{0,\gamma} = \int_\omega w(r)\, v^2 \,\mathrm{d}\Omega.$$

Above, the weight w is a function of the distance to the reentrant edges, namely $w(r) = \min(r^{2\gamma}, 1)$, with for instance $\gamma = 0.99$ (one may choose $\gamma \in [0, 1]$). Notice that this definition is slightly different than the general one given in [13]. $H^1(\Omega)$ will denote the space of $L^2(\Omega)$ functions with gradients in $L^2(\Omega)^3$. We now define variational spaces for vector fields, together with the associated norms:

$$\mathcal{H}(\mathbf{curl}, \Omega) := \{\mathcal{F} \in L^2(\Omega)^3 \,|\, \mathbf{curl}\mathcal{F} \in L^2(\Omega)^3\},\ ||\mathcal{F}||^2_{0,\mathbf{curl}} = ||\,\mathcal{F}\,||^2_0 + ||\mathbf{curl}\mathcal{F}||^2_0\,,$$
$$\mathcal{H}(\mathrm{div}_{(\gamma)}, \Omega) := \{\mathcal{F} \in L^2(\Omega)^3 \,|\, \mathrm{div}\mathcal{F} \in L^2_{(\gamma)}(\Omega)\},\ ||\mathcal{F}||^2_{0,\mathrm{div}_{(\gamma)}} = ||\,\mathcal{F}\,||^2_0 + ||\mathrm{div}\mathcal{F}||^2_{0(,\gamma)}\,.$$

The index $_{(\gamma)}$ means that one can choose to use weights or not.
Under suitable data assumptions, $\mathcal{E} \in \mathcal{X}^A_{\mathcal{E}(,\gamma)}$, with:

$$\mathcal{H}_A(\mathbf{curl}, \Omega) := \{\mathcal{F} \in \mathcal{H}(\mathbf{curl}, \Omega) \,|\, \mathcal{F} \times \mathbf{n}_{|\partial\Omega} \in \mathcal{L}^2_t(\partial\Omega)\,,\ \mathcal{F} \times \mathbf{n}_{|\Gamma_C} = 0\},$$
$$\mathcal{X}^A_{\mathcal{E}(,\gamma)} := \mathcal{H}_A(\mathbf{curl}, \Omega) \cap \mathcal{H}(\mathrm{div}_{(\gamma)}, \Omega),$$

where $\mathcal{L}^2_t(\partial\Omega) := \{\mathbf{u} \in L^2(\partial\Omega)^3 \,|\, \mathbf{u} \cdot \mathbf{n} = 0 \text{ a. e.}\}$. When $\Gamma_C = \partial\Omega$, we write simply $\mathcal{X}^0_{\mathcal{E}(,\gamma)}$.
According to Costabel [12], and to Costabel-Dauge [13], the graph norm and the semi-norm: $||\mathcal{F}||^2_{\mathcal{X}^0_{\mathcal{E}(,\gamma)}} = ||\mathbf{curl}\mathcal{F}||^2_0 + ||\mathrm{div}\mathcal{F}||^2_{0(,\gamma)}$ are equivalent on $\mathcal{X}^0_{\mathcal{E}(,\gamma)}$. Note that, when there is a weight, this is true only if $\gamma < 1$. Moreover, $\exists \gamma_{min} \in]0, 1[$ such that for all $\gamma \in]\gamma_{min}, 1[$, $\mathcal{X}^0_{\mathcal{E},\gamma} \cap H^1(\Omega)^3$ is dense in $\mathcal{X}^0_{\mathcal{E},\gamma}$.

2 Variational formulations and discretization

Starting from the second order system of eqs. (9-13), we obtain a series of variational formulations, retracing the steps below:
- Multiply eq. (9) by $\mathcal{F} \in \mathcal{H}_A(\mathbf{curl}, \Omega)$, and integrate by parts over Ω. We get the variational formulation (VF): *Find* $\mathcal{E}(t) \in \mathcal{H}_A(\mathbf{curl}, \Omega)$ *such that* $\forall \mathcal{F} \in \mathcal{H}_A(\mathbf{curl}, \Omega)$, $\forall t$,

$$(\mathcal{E}'', \mathcal{F})_0 + c^2(\mathbf{curl}\mathcal{E}, \mathbf{curl}\mathcal{F})_0 + c \int_{\Gamma_A} (\mathcal{E}' \times \mathbf{n}).(\mathcal{F} \times \mathbf{n})\,\mathrm{d}\Gamma$$
$$= -(\mathcal{J}'/\varepsilon_0, \mathcal{F})_0 + \int_{\Gamma_A} (c\mathbf{b}' \times \mathbf{n}).\mathcal{F}\,\mathrm{d}\Gamma\,, \qquad (14)$$

- Add $c^2(\mathrm{div}\mathcal{E}, \mathrm{div}\mathcal{F})_{0(,\gamma)}$ on the LHS and $c^2(\rho/\varepsilon_0, \mathrm{div}\mathcal{F})_{0(,\gamma)}$ on the RHS to get the augmented VF (AVF): *Find* $\mathcal{E}(t) \in \mathcal{X}^A_{\mathcal{E}(,\gamma)}$ *such that* $\forall \mathcal{F} \in \mathcal{X}^A_{\mathcal{E}(,\gamma)}$, $\forall t$,

$$(\mathcal{E}'',\mathcal{F})_0 + c^2(\mathcal{E},\mathcal{F})_{\mathcal{X}^0_{\mathcal{E}(,\gamma)}} + c\int_{\Gamma_A}(\mathcal{E}'\times\mathbf{n}).(\mathcal{F}\times\mathbf{n})\,\mathrm{d}\Gamma$$
$$= -(\mathcal{J}'/\varepsilon_0,\mathcal{F})_0 + c^2(\rho/\varepsilon_0,\mathrm{div}\mathcal{F})_{0(,\gamma)} + \int_{\Gamma_A}(c\mathbf{b}'\times\mathbf{n}).\mathcal{F}\,\mathrm{d}\Gamma\,, \qquad (15)$$

- Add $(p,\mathrm{div}\mathcal{F})_{0(,\gamma)}$ on the LHS and consider a constraint on the divergence of $\mathcal{E}$ (cf. (17)). If $p\in L^2_{(\gamma)}(\Omega)$ is the Lagrange multiplier, we reach the mixed AVF (MAVF): *Find* $(\mathcal{E}(t),p(t))\in\mathcal{X}^A_{\mathcal{E}(,\gamma)}\times L^2_{(\gamma)}(\Omega)$ *such that* $\forall\mathcal{F}\in\mathcal{X}^A_{\mathcal{E}(,\gamma)}$, $\forall t$,

$$(\mathcal{E}'',\mathcal{F})_0 + c^2(\mathcal{E},\mathcal{F})_{\mathcal{X}^0_{\mathcal{E}(,\gamma)}} + (p,\mathrm{div}\mathcal{F})_{0(,\gamma)} + c\int_{\Gamma_A}(\mathcal{E}'\times\mathbf{n}).(\mathcal{F}\times\mathbf{n})\,\mathrm{d}\Gamma$$
$$= -(\mathcal{J}'/\varepsilon_0,\mathcal{F})_0 + c^2(\rho/\varepsilon_0,\mathrm{div}\mathcal{F})_{0(,\gamma)} + \int_{\Gamma_A}(c\mathbf{b}'\times\mathbf{n}).\mathcal{F}\,\mathrm{d}\Gamma\,, \qquad (16)$$

and $\forall q\in L^2_{(\gamma)}(\Omega)$, $\forall t$,

$$(\mathrm{div}\mathcal{E},q)_{0(,\gamma)} = (\rho/\varepsilon_0,q)_{0(,\gamma)}\,. \qquad (17)$$

The constraint (17) is added to reinforce Gauss' law (3) and also to avoid numerical instabilities when the discrete charge conservation equation is not satisfied while solving the Maxwell-Vlasov system [5].

Theorem 1. *Suppose that* $\partial_t\mathcal{J}\in L^2(0,T;L^2(\Omega)^3)$, $\partial_t\rho\in L^2(0,T;L^2_{(\gamma)}(\Omega))$, ρ *and* $\mathcal{J}$ *satisfying (5). Suppose that* $(\mathcal{E}_0,\mathcal{E}_1)\in\mathcal{X}^A_{\mathcal{E}(,\gamma)}\times L^2(\Omega)^3$. *Then, equations (16-17) are equivalent to problem (PE) and have a unique solution* $(\mathcal{E},p)$ *such that* $(\mathcal{E},\partial_t\mathcal{E})\in C^0(0,T;\mathcal{X}^A_{\mathcal{E}(,\gamma)})\times C^0(0,T;L^2(\Omega)^3)$ *and* $p=0$.

The proof can be found in [16]. Idem for the magnetic field.

To build a discretized (M)AVF, we use a leap-frog scheme in time, and either the continuous P_k Lagrange FE (no Lagrange mutliplier) or the P_{k+1}-P_k continuous Taylor-Hood FE in space. We choose an explicit scheme. Let Δt be the time step and $t_n = n\Delta t$, $n\in\mathbb{N}$. $u''(.,t_{n+1})$ is approximated by: $u''(.,t_{n+1})\approx[u(.,t_{n+1})-2u(.,t_n)+u(.,t_{n-1})]/\Delta t^2$. Recall that for an explicit scheme, one must satisfy a CFL-like condition. For the P_1 FE, we must have: $\Delta t\leq 0.5\,c\,\min_l h_l$, where h_l is the diameter of the l^{th} tetrahedron. Let N_k (resp. N_{k+1}) be the number of P_k (resp. P_{k+1}) degrees of freedom.
Let $\mathrm{E}^n\in(\mathbb{R}^3)^{\mathrm{N}_{k+1}}$ be the discretized electric field and $\mathrm{p}^n\in\mathbb{R}^{\mathrm{N}_k}$ be the discretized Lagrange multiplier at time t_n. Let $\mathbb{M}_\Omega\in(\mathbb{R}^{3\times3})^{\mathrm{N}_{k+1}\times\mathrm{N}_{k+1}}$ be the mass matrix, and $\mathbb{M}^{\|}_{\Gamma_A}\in(\mathbb{R}^{3\times3})^{\mathrm{N}_{k+1}\times\mathrm{N}_{k+1}}$ be the boundary mass matrix on Γ_A. Let $\mathbb{C}\in(\mathbb{R}^{1\times3})^{\mathrm{N}_k\times\mathrm{N}_{k+1}}$ be the constraint matrix. At a given time t_{n+1}, $n\in\mathbb{N}$, we have to solve:

$$\begin{aligned}(\mathbb{M}_\Omega + c\Delta t\mathbb{M}^{\|}_{\Gamma_A})\mathrm{E}^{n+1} + \mathbb{C}^T\mathrm{p}^{n+1} &= \mathrm{RHS}^{n+1}\,,\\ \mathbb{C}\mathrm{E}^{n+1} &= \mathrm{G}^{n+1}\,.\end{aligned} \qquad (18)$$

Let $\mathbb{M} = \mathbb{M}_\Omega + c\Delta t \mathbb{M}^{\parallel}_{\Gamma_A}$. The algorithm is the following:
Solve first $\mathbb{M}\mathrm{E}_0^{n+1} = \mathrm{RHS}^{n+1}$, then $\mathbb{C}\mathbb{M}^{-1}\mathbb{C}^T\mathrm{p}^{n+1} = \mathbb{C}\mathrm{E}_0^{n+1} - \mathrm{G}^{n+1}$, and finally $\mathbb{M}\mathrm{E}^{n+1} = \mathbb{M}\mathrm{E}_0^{n+1} - \mathbb{C}^T\mathrm{p}^{n+1}$. The Lagrange multiplier p^{n+1} may be computed with the Uzawa algorithm. Note that when there is no coupling with Vlasov equation, p^{n+1} remains small at all times, so that there is actually no need to compute it at all times. To speed up the resolution, one can lump $\mathbb{M}$ with $\widetilde{P}_1$ or $\widetilde{P}_2$ FE [11]. Both $\widetilde{P}_k$ FE preserve accuracy, at the cost of increasing the total number of degrees of freedom for the $\widetilde{P}_2$ FE.

3 Numerical results and conclusion

The numerical results are given for the following model problem (fig. 1): Ω has a single reentrant edge of dihedral angle $2\pi/3$, so that $\alpha = 2/3$. A current bar crosses the domain, with $\mathcal{J} = 10^{-5}\omega \sin(\pi z/L)\cos(\omega t)\mathbf{z}$ and $\rho = 10^{-5}(\pi/L)\cos(\pi z/L)\sin(\omega t)$, for $\omega = 2.5$ GHz. There is no incoming wave. The spatial wavelength associated to ω is of order 0.75 m, and the time period is of order 2.5 ns. It is clear that the dimensions of our domain are not realistic, however we made this choice in order to visualize oscillations. We report the results of computations made with the $\widetilde{P}_1$ FE (discretization of the AVF), and with 685 000 tetrahedra. We encoded the problem in Fortran 77.

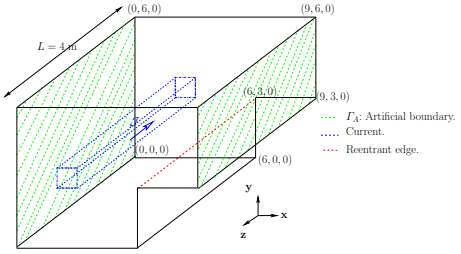

Fig. 1. The model problem.

On figures 2 and 3 the space evolution of the x and y-components of the electric field are represented in the plane $z = 2.5$ m, at times $T_1 = 1$ ns, $T_2 = 8$ ns, $T_3 = 15$ ns, $T_4 = 20$ ns. We can see that an electric wave is created by the current, that it propagates into the cavity with wavelength ≈ 0.75 m, and is reflected by the conductor as expected. At T_3, we observe a growing peak of intensity close to the reentrant corner.
On figure 4, we represented the space evolution of the z-component in the plane $z = 2.5$ m, at times T_i, $i = 1, 4$. Again, we observe the propagation of the wave with wavelength ≈ 0.75 m, and the reflections. Note that this component has a regular behaviour, which is due to the fact that the only geometrical singularity is along the z-axis [7, 9]. Moreover, it takes smaller

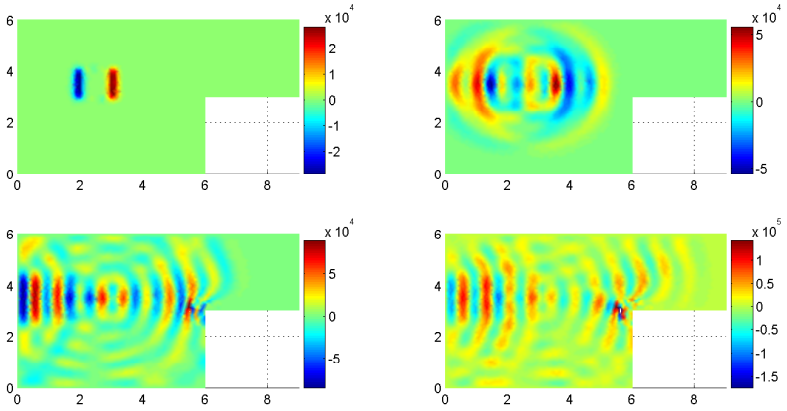

Fig. 2. $\mathrm{E}_x^{\tilde{P}_1}$ component at times T_i, $i = 1$ to 4, in plane $z = 2,5$ m.

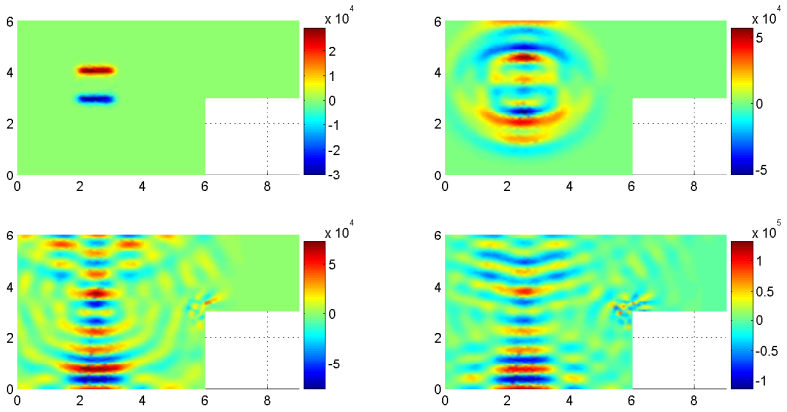

Fig. 3. $\mathrm{E}_y^{\tilde{P}_1}$ component at times T_i, $i = 1$ to 4, in plane $z = 2,5$ m.

(absolute) values than the x and y-components.
On figures 2, 3 and 4, one can see spurious reflections on Γ_A, due to the fact that the Silver-Müller boundary condition is simply of first order: only plane waves with normal incidence are absorbed, which is not our case. In addition, the spurious reflections appear more important for E_x than for E_y, since its values are more intense horizontally.
On figure 5, we present the time evolution of the x-component of the electric field at points $M_1 = (1,1,2)$, $M_2 = (5.5,2.5,2)$, $M_3 = (1,1,2)$, $M_4 = (8,5.5,2)$. It remains equal to zero until the electric wave reaches the point under consideration. Then the field oscillates with a period ≈ 2.5 ns, as expected.

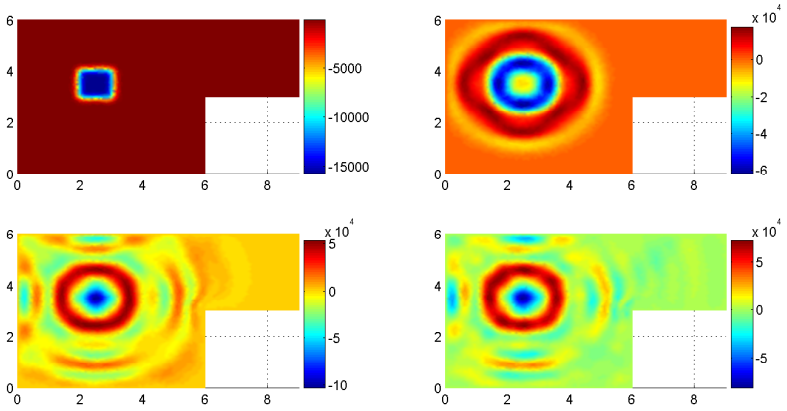

Fig. 4. $\mathrm{E}_z^{\widetilde{P}_1}$ component at times T_i, $i = 1$ to 4, in plane $z = 2,5$ m.

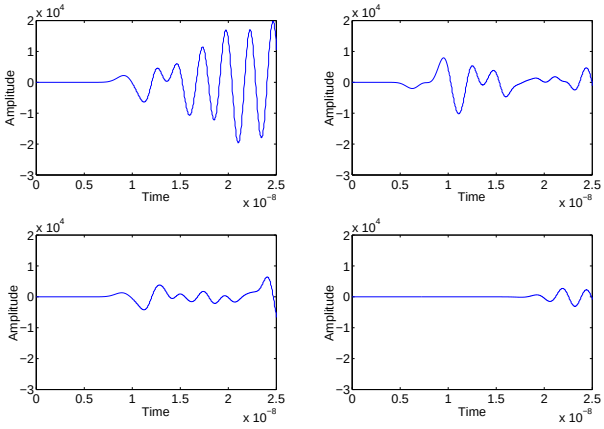

Fig. 5. $\mathrm{E}_x^{\widetilde{P}_1}$ component at points M_i, $i = 1$ to 4.

To the authors' knowledge, this is the first time a $3D$ singular electric field is computed with continuous Lagrange FE. According to M. Dauge (private communication), the WRM can also be used to compute the magnetic field, with similar assumptions on γ. In order to avoid spurious reflections, we suggest to use perfectly matched layers [6]. For the resolution of $2D$ Maxwell equations with continuous Galerkin finite elements, we refer the reader to [10].

References

1. Assous, F., Degond, P., Heintzé, E., Raviart, P.-A., Segré, J.: On a finite element method for solving the three-dimensional Maxwell equations. J. Comput. Phys., **109**, 222–237 (1993)
2. Assous, F., Ciarlet, Jr, P., Labrunie, S., Segré, J.: Numerical solution to the time-dependent Maxwell equations in axisymmetric singular domains: The Singular Complement Method. J. Comput. Phys., **191**, 147–176 (2003)
3. Assous, F., Ciarlet, Jr, P., Segré, J.: Numerical solution to the time-dependent Maxwell equations in two-dimensional singular domains: the singular complement method. J. Comput. Phys., **161**, 218–249 (2000)
4. Assous, F., Ciarlet, Jr, P., Sonnendrücker, E.: Resolution of the Maxwell equations in a domain with reentrant corners. Modél. Math. Anal. Numér., **32**, 359–389 (1998)
5. Barthelmé, R.: Le problème de conservation de la charge dans le couplage des équations de Maxwell et de Vlasov. PhD thesis, Université Strasbourg I, France (2005)
6. Bérenger, J.-P.: A perfectly matched layer for the absorption of electromagnetic waves. J. Comput. Phys., **114**, 185–200 (1994)
7. Buffa, A., Costabel M., Dauge M.: Anisotropic regularity results for Laplace and Maxwell operators in a polyhedron. C. R. Acad. Sci. Paris, Ser I, **336**, 565–570 (2003)
8. Ciarlet, Jr, P.: Augmented formulations for solving Maxwell equations. Comp. Meth. Appl. Mech. and Eng., **194**, 559–586 (2005)
9. Ciarlet, Jr, P., Garcia, E., Zou, J.: Solving Maxwell equations in $3D$ prismatic domains. C. R. Acad. Sci. Paris, Ser. I, **339**, 721–726 (2004)
10. Ciarlet, Jr, P., Jamelot, E.: A comparison of nodal finite element methods for solving Maxwell equations. *In preparation.*
11. Cohen, G.: Higher-Order Numerical Methods for Transient Wave Equations. Scientific Computation Series. Springer-Verlag, Berlin (2002)
12. Costabel, M.: A coercive bilinear form for Maxwell's equations. J. Math. An. Appl., **157**, 527–541 (1991)
13. Costabel, M., Dauge, M.: Weighted regularization of Maxwell equations in polyhedral domains. Numer. Math., **93**, 239–277 (2002)
14. Garcia, E.: Solution to the instationary Maxwell equations with charges in non-convex domains (in French). PhD thesis, Université Paris VI, France (2002)
15. Jamelot, E.: Éléments finis nodaux pour les équations de Maxwell. C. R. Acad. Sci. Paris, Sér. I, **339**, 809–814 (2004)
16. Jamelot, E.: Solution to Maxwell equations with continuous Galerkin finite elements (in French). PhD thesis, École Polytechnique, Palaiseau, France (2005)